Desalination and Water Treatment
www.deswater.com

doi: 10.1080/19443994.2014.896750

54 (2015) 2270–2279
May

Optimization of process parameters during photocatalytic degradation of phenol in UV annular reactor

Sangita Bhattacharjee[a], Sudip Chakraborty[b,c], Kunal Mandol[a], Lei Liu[d], Heechul Choi[d], Chiranjib Bhattacharjee[b,*]

[a]*Chemical Engineering Department, Heritage Institute of Technology, Kolkata, India*
[b]*Chemical Engineering Department, Jadavpur University, Kolkata, India, Tel. +91 98364 02118;*
email: cbhattacharyya@chemical.jdvu.ac.in
[c]*Department of Chemical Engineering and Materials, University of Calabria, Cubo-44A, 87036 Rende (CS), Italy*
[d]*School of Environmental Science and Engineering, Gwangju Institute of Science and Technology (GIST), 261 Cheomdan-gwagiro, 1 Oryong-dong, Buk-gu, Gwangju, 500-712, South Korea*

Received 25 October 2013; Accepted 18 February 2014

ABSTRACT

In this work, photocatalytic oxidation of aqueous phenol solution was carried out in a novel UV-irradiated annular reactor in the presence of TiO_2 catalyst. The photocatalytic experiments were conducted by varying the flow rates (5, 7.5, and 10 LPH), substrate-to-catalyst ratios (0.083, 0.5415, and 1), and solution pH (3, 6, and 9). In each case, the demineralization of phenol in aqueous was investigated after an operating time of 3 h. The influence of each parameter on phenol degradation was thoroughly investigated and reported. The strategy consisted of several steps, such as selection of the variables and their experimental domain, use of a screening design to detect significant variables and interactions into the experimental region, study of the main effect of variables and interactions, and finally application of a Draper–Lin small composite design (orthogonal) to obtain the optimum values of the significant variables leading to high conversion of phenol. Efficiency of phenol degradation was found to decrease with increase in substrate to TiO_2 ratio. The flow rate and solution pH were found to affect the degradation appreciably. Kinetic study of the photocatalytic reaction revealed that phenol degradation could be well explained using Langmuir–Hinshelwood model. In dilute solution, the degradation was found to follow a pseudo-first-order model. The apparent rate constant was determined and reported.

Keywords: Photocatalytic oxidation; UV; Phenol conversion; TiO_2 dosage; Draper–Lin small composite designs; Langmuir–Hinshelwood model

1. Introduction

Heterogeneous photocatalysis is a "green" technology with potential applications in various disciplines, such as chemical synthesis and environmental technologies. These processes use certain metal oxides that can generate hydroxyl radicals on the surfaces of particles when exposed to UV light. The anatase form of TiO_2 has low band-gap energy (approximately 3.2 eV), which is almost equivalent to 400 nm wavelength of light. Activation of semiconductor TiO_2 catalyst

---

*Corresponding author.

achieved through the absorption of photon of ultraviolet band-gap energy, results in the formation of electron donor (reducing) and electron acceptor (oxidising) sites. The photocatalytic activity of TiO_2 depends on the relative rates of generation and recombination of electron-hole pairs as well as the adsorption of radical-forming species on TiO_2 surfaces. Hydroxyl radicals (HO•) and superoxide ions are the principal agents responsible for the oxidation of aqueous organic contaminants [1]. The carbon-containing pollutants are oxidized to carbon dioxide and water, while the other elements bonded to the organic compounds are converted to anions, such as nitrate, sulfate, or chloride.

The purification of wastewater by heterogeneous photocatalysis is one of the most rapidly growing areas of interest to both research workers and water purification plants. Commercial application of the process is called advanced oxidation process (AOP). In recent years, TiO_2 has been chosen as a photocatalyst for the destruction of polluting materials due to its efficiency, non-toxicity, high activity, photochemical inertness, and low cost [2]. In some recent work, photocatalytic degradation of reactive Black-5 (RB-5) dye using TiO_2-impregnated ZSM-5 has been investigated in a batch reactor [3]. With some optimum formulation of supported catalyst, 98% degradation of 50 mg/L RB-5 solutions was obtained in 90 min. Hosseinia et al. [4] had synthesized nanosize TiO_2 particles, and investigated photocatalytic degradation of different chromophores under visible light irradiation at different catalyst loading and different dye concentrations. In another work [5], phenol degradation had been examined with combined photocatalysts TiO_2 and ZnO under illumination of a 500 W super high-pressure mercury lamp mounted axially. The results revealed that, both TiO_2 and ZnO were effective, though the latter was much superior in terms of photocatalytic activity. Photocatalysis has been found to be particularly useful for cleaning biologically toxic or non-biodegradable materials, such as aromatics, pesticides, petroleum constituents, dyes, and volatile organic compounds in wastewater [6].

The effluents of various chemical and pharmaceutical industries, coal refineries, phenol manufacturing, pharmaceuticals, dying, petrochemical, pulp mill etc. include wide variety of organic chemicals like phenol and various substituted phenols. Phenol is one of the most prevalent chemical and pharmaceutical pollutants, due to its toxicity even at lower concentrations and formation of substituted compounds during oxidation and disinfection processes. Its direct effect on the environment include depletion of ozone layer, the earth's heat balance, reduced visibility, and addition of acidic air pollutants to the atmosphere [7]. Phenol removal from the industrial wastewater is utmost necessary, as phenol concentration in wastewater inhibits or eliminates micro-organisms, thus strongly reducing the biodegradation of other components. Accordingly, efforts are being given to reduce phenol concentration prior to the wastewater discharge, so as to decrease all these detrimental effects. Various methods have been suggested so far to degrade phenol effectively using AOP [8,9]. The advantages of these processes are that these lead to the total mineralization of organic contaminants.

A number of photocatalytic reactors have been patented in recent years, but none have so far been developed in pilot scale. In light of the above discussion, the work in this paper was undertaken to study photocatalysis of phenol in aqueous using TiO_2 as catalyst in an indigenously designed UV-irradiated annular reactor. Effects of influencing parameters, such as flow rate, reactor operating time, solution pH, catalyst loading, etc. on degradation of phenol were investigated in detail. The model proposed by Langmuir–Hinshelwood (L–H) was employed to describe the kinetics of the photodecomposition reaction of phenol in the proposed semi-batch reactor, and the rate constant was evaluated under specified operating conditions. Efforts have been given to optimize the system parameters with an objective to maximize the phenol degradation.

In many cases, the purpose of an experiment is to optimize the response or to achieve a desirable value of the response. Assuming the system or process involves a response y_y that depends on the k_k input factors $x_1, x_2, \ldots, x_k$ through an unknown function ff (i.e. $y = f(x_1, x_2, \ldots x_k)$. Response surface methodology (RSM) aims at investigation and approximation of the unknown function ff using experimentation, modeling, and data analysis. The common way that researchers address RSM in the literature is to use central composite designs (CCD), suggested by Box and Wilson [10], or small composite designs (SCD) proposed by Draper and Lin [11]. Because of the presence of four components in this study, three independent variables and one dependent variable, a substantial number of experiments should be simultaneously executed, and their possible interactions also should be studied. For this reason, the authors applied a highly efficient optimization method with the experimental studies. The proposed Draper–Lin SCD was used to develop mathematical models, with an objective to estimate the relationships between the response and the key independent variables as well as to determine the optimum conversion of phenol using TiO_2 nanoparticle.

2. Photocatalytic degradation of phenol

The heterogeneous photocatalysis allows total degradation (mineralization) of the most toxic organic molecules in aqueous solution in the presence of a catalyst. In this process, excitation of TiO_2 by a UV light of wavelength $\lambda \leq 380$ nm generates electron-hole pairs ($e^-_{cb}\,h^+_{vb}$). Dissolved oxygen of the solution scavenges the electron generated, preventing the recombination of electrons and holes. Conduction band electrons and valence band holes generated from UV-irradiated TiO_2 (Eq. (1)) interact with TiO_2 surface-adsorbed-molecular-oxygen and water to generate superoxide radical $O_2\cdot$ (Eq. (2)), and the highly reactive $HO\cdot$, respectively (Eqs. (2) and (3)). The hydroxyl radicals generated in this process are powerful oxidants due to their high reactivity [1]. This species is unstable and is continuously produced due to photochemical reactions. The mechanism of the photocatalysis [1] is shown below through Eq. (1)–(4):

$$TiO_2 + h\upsilon \rightarrow e^-_{cb} + h^+_{vb} \tag{1}$$

$$e^-_{cb} + O_2(\text{ads}) \rightarrow O_2^- \tag{2}$$

$$h^+_{vb} + H_2O \rightarrow HO^{\cdot}_{ads} + H^+ \tag{3}$$

$$HO^{\cdot}_{ads} + \text{Reactants} \rightarrow \text{Photooxidized} - \text{products} \tag{4}$$

The photo-degradation efficiency or conversion was calculated by the following relation (Eq. (5)):

$$X(\%) = 100 \times (C_0 - C)/C_0 \tag{5}$$

where X is the photo-degradation efficiency or conversion.

3. Experimental materials and methods

3.1. Reagents

The catalyst TiO_2 (more than 99.9% purity) was procured from Sigma, Aldrich and was used without any pre-treatment. From XRD analysis, it was found that (Fig. 1) TiO_2 contained only anatase form. Phenol with a purity > 99.9 % was also obtained from Merck, India. The aqueous solutions were prepared with deionized water. The ultra-pure deionized water used in this study was obtained from the Arium RO unit followed by Arium 611DI ultrapure water system (Sartorius, Göttingen, Germany).

3.2. Calibration curve

Dilute solutions with six different concentrations of phenol were prepared for construction of standard curve. Aqueous phenol solution was scanned for maximum absorbance, and was found to give peak absorbance (λ_{max}) at 270 nm in a UV–visible VARIAN UV–visible spectrophotometer (Cary50 Bio). The absorbance vs. concentration data were plotted and this curve was used to determine phenol concentration during subsequent experimental runs.

3.3. Photoreactor

The photoreactor of capacity 1,720 mL contained 305 mm long, four UV lamps, each of 50 W. The sources of irradiation were placed uniformly inside the reactor to assure maximum energy exchange between the source of irradiation and reaction mixture that would flow continuously. A pump was used to circulate the mixture between the reactor and the reservoir containing the feed solution. The schematic diagram of the experimental setup is furnished in Fig. 2.

3.4. Experimental procedure

Phenol solution (5 L) of desired concentration was prepared by accurately measuring phenol in an electronic weighing balance (supplied by Sartorius, India Ltd.), and dissolving in deionized water. Specified amount of TiO_2 was accurately weighed and was mixed thoroughly with the phenol solution in the feed reservoir. The suspension was stirred for about one hour in the absence of UV light in order to reach adsorption equilibrium before irradiation with UV light. Photocatalysis reaction was carried out for a period of 3 h for each of the three flow rates of 5, 7.5, and 10 LPH, respectively, using different phenol concentrations (50, 125, and 200 ppm, respectively). The solution coming out of the reactor was directed to the reservoir and was allowed to mix thoroughly with the solution. During experiment, the temperature of the phenol solution in the reservoir was kept constant at 32 ℃ with the help of a temperature controller. Each experiment was repeated thrice and average value of phenol concentration was used for calculating conversion. The sample of reaction suspension (5 mL) was withdrawn with a syringe from the reservoir at regular intervals of 30 min. Each sample collected was then filtered using 0.45 μm polyethersulphone (Millipore) membranes and then analyzed in the VARIAN UV spectrophotometer by measuring the absorbance at 270 nm. Using the calibration curve, the remaining phenol concentration of the sample was determined.

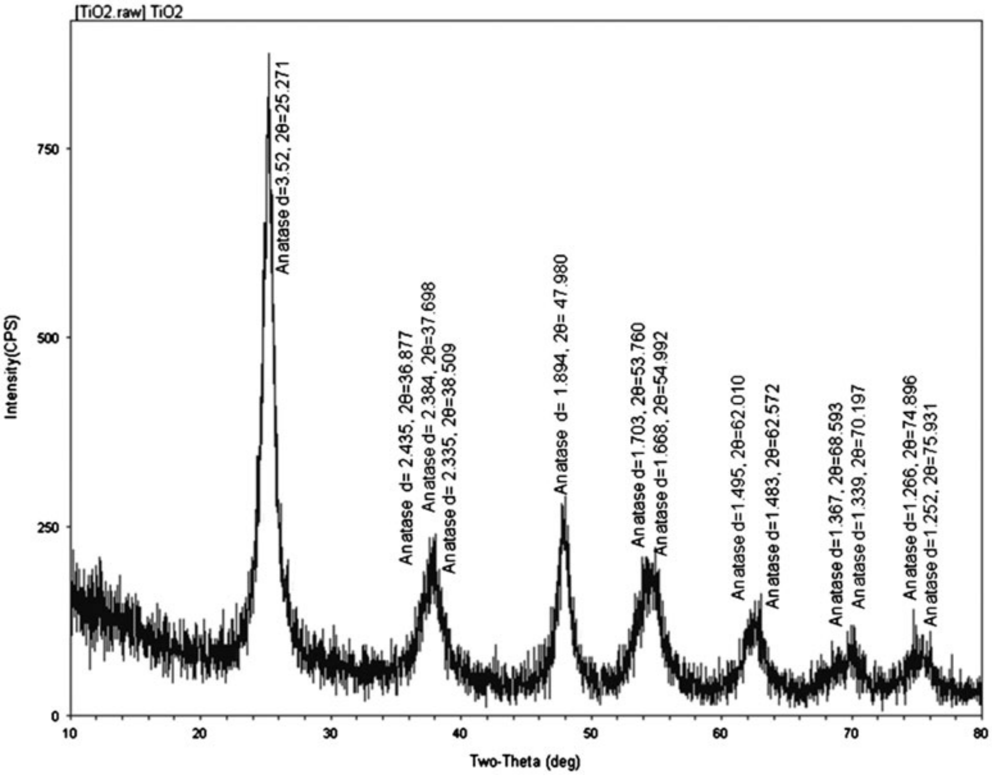

Fig. 1. XRD analysis of TiO_2.

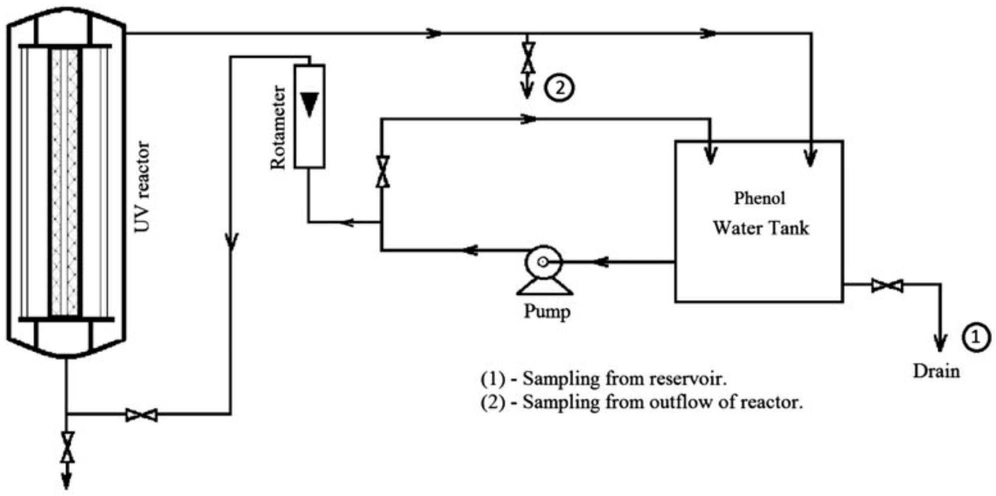

Fig. 2. Schematic diagram of annular UV photo reactor.

3.5. Draper–Lin SCD

As a collection of statistical and mathematical techniques, RSM is useful for developing, improving, and optimizing processes [12,13]. The relationship among the significant variables would be expressed in a second-order equation (Eq. (6)):

$$Y_k = \beta_0 + \sum \beta_i x_i + \sum \beta_{ii} x_i^2 + \sum \sum_{i \neq j} \beta_{ij} x_i x_j + \varepsilon \tag{6}$$

where Y_k is the predicted response, β_0 is the constant, β_i is the linear effect, β_{ii} is the squared effect, and β_{ij} is the interaction effect, and ε is an experimental error. The parameters x_i and x_j represent the independent variables (medium components) in the form of coded values as follows (Eq. (7)):

$$x_i = \frac{X_i - X}{\Delta X_i} \tag{7}$$

where x_i and X_i are the dimensionless and the actual values of independent variable *i*, X is the actual value of the independent variable *i* at the central point, and ΔX_i is the step change of X_i corresponding to a unit variation of the dimensionless value.

In this article, a Draper–Lin SCD was used to optimize three independent variable parameters which influence the phenol conversion with TiO_2 as a photocatalyst. The levels of variables are shown in Table 1. The extreme level of axial points was chosen to be 1.861 in order to make this design rotatable [14,15]. The experimental runs were randomized in order to exclude the block effects. Once the responses were obtained, the analysis of variance was carried out. This well-known statistical technique can be used to separate any variation caused by changing a controlled factor from the variation due to random error.

3.5. Kinetic studies

The L–H kinetic model was used to describe the mineralization process kinetics. The L–H model was initially developed to quantitatively describe gaseous–solid reactions [4], but recently employed to describe solid–liquid reactions. In this model, the rate of reaction (*r*) is proportional to the fraction of surface covered by the substrate (θ), as shown below in Eq. (8):

$$r = -dc/dt = k_r \theta \tag{8}$$

Considering Langmuir's equation (Eq. (9)),

$$\theta = KC/(1 + KC) \tag{9}$$

Combining Eq. (8) and (9),

$$r = k_r KC/(1 + KC) \tag{10}$$

In Eq. (10) k_r is the true rate constant, K is the Langmuir constant, and C is the concentration of the organic substrate at any time *t*. Since in this case, the solution is highly diluted, C (mol/L)$<10^{-3}$ [15] the term KC becomes <<1, and the reaction transforms to an apparent first-order reaction, whose kinetic expression may be written as follows (Eq. (11)):

$$r = -dc/dt = k_r KC = k_{app} C \tag{11}$$

where k_{app} is the apparent rate constant of a pseudo-first-order reaction.

Integrating and using boundary condition $C = C_0$ at $t = 0$,

$$\ln(C_0/C) = k_{app} \times t \tag{12}$$

Hence, by plotting ln (C_0/C) against time (as shown in Eq. (12)), the apparent rate constant can be found out from the slope of the line.

Table 1
Range and levels of independent variables (as per Draper–Lin SCD)

	Operating parameters (independent variable)		
Range of measured value	Operating time (h) X_1	Flow rate (LPH) X_2	Substrate-to-catalyst ratio X_3
Low range	0	5	0.083
Middle range	1.5	7.5	0.458
High range	3	10	1.0

4. Results and discussion

The influences of different parameters on photocatalytic degradation of phenol were investigated in detail. Through graphical presentations and RSM analysis, the results have been described in this section. To cut down the number of runs and increase the efficiency, the Draper–Lin SCD was developed [11]. SCD had been applied and considered as a highly efficient statistical experimental design tool in chemical engineering optimization [16]. Optimization of different operating parameters was done by fitting the quadratic polynomial model (as explained through Eq. (6)), and high R^2 value of 96.2879 showed goodness of fit in terms of variability in the phenol conversion. The standard error of the estimate was represented in terms of the standard deviation of the residuals, which was found to be 0.37131. The residual analysis, which is generally used to establish any possible significant correlation, was carried out with the Durbin–Watson (DW) statistical tests and showed a lower *F*-ratio value, equal to 1.95 ($p = 0.2239$). There is no indication of serial autocorrelation in the residuals at the 5.0% significance level. Since the *F*-ratio of lack of fit shows a lower value, equal to 5.11 ($p = 0.0253$), the model appears to be adequate for the observed data at the 95% confidence level.

In this case, three effects have *p*-values less than 0.05, indicating that they are significantly different from zero at the 95.0% confidence level. Fig. 3 shows the linear, quadratic, and interaction values of each factor investigated and plotted in the form of a Pareto chart, where the effect is significant if its corresponding bar crosses the vertical line at the $p = 0.05$ level. The quadratic effect of pH was found to be the most significant effect ($p \leq 0.05$) to produce variability in the phenol conversion, followed by the quadratic effect of pH, quadratic effect of flow rate and catalyst load. The response surface of the phenol conversion is plotted against two operating variables, while the third variable is kept constant. The 3D plot (Fig. 4 was obtained using Eq. (6) and shows the effect of different operating parameters on phenol conversion by photocatalytic reaction. The *R*-Squared statistic indicates that the model as fitted explains 84.49% of the variability in Phenol Degradation. The adjusted *R*-squared statistic, which is more suitable for comparing models with different numbers of independent variables, is 82.74%. The standard error of the estimate shows the standard deviation of the residuals to be 2.11. The mean absolute error of 1.48 is the average value of the residuals. The DW statistic tests the residuals to determine if there is any significant correlation based on the order in which they occur in the data file. Since the *p*-value is less than 5.0%, there is an indication of possible serial correlation at the 5.0% significance level.

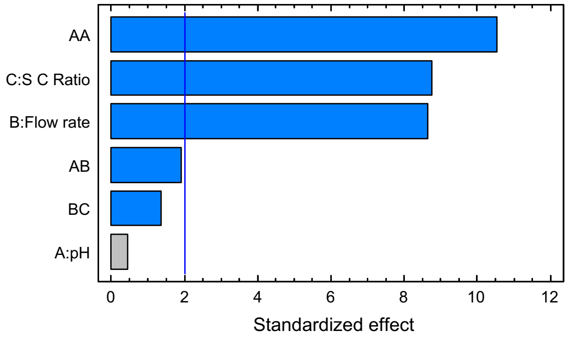

Fig. 3. Standardized Pareto chart for phenol conversion.

4.1. Effect of flow rate

Adsorption and photo-degradation of phenol was carried out with varying flow rates 5, 7.5, and 10 LPH, respectively. The conversion of phenol was plotted against time by measuring the residual phenol concentration in solution. From the experimental study, it was observed that highest conversion (52.81%) had been achieved at a flow rate of 5 LPH which was further corroborated through statistical analysis. The increase in percent degradation of phenol at lower flow rate could be due to enhanced residence time and higher exposure to UV irradiation in the UV–annular reactor. Turbulence also might have some effect on the conversion of phenol at higher flow rate; the effect is not so pronounced as all the experimental runs were carried out keeping TiO_2 nanoparticles in suspension. Had it been carried out using TiO_2 nanoparticles in immobilized form on some substrate, turbulence would have a greater effect in controlling the conversion of phenol by reducing the diffusional mass transfer resistance from the bulk solution to the catalyst surface (Fig. 4(d)).

4.2. Effect of substrate concentration and catalyst doses (S/C ratio)

The effect of the ratio of initial phenol concentration (50, 125, and 200 mg/L) to catalyst loading (200, 400, and 600 mg/L) on phenol degradation by the UV/TiO_2 process was investigated. Accordingly, the Substrate-to-catalyst ratio (S/C ratio) varied from 0.083 (minimum) to 1.0 (maximum). Fig. 4(a) shows the interaction of flow rate and S/C ratio on phenol degradation. With increase in S/C ratio at constant flow rate resulted in decrease of phenol degradation which may

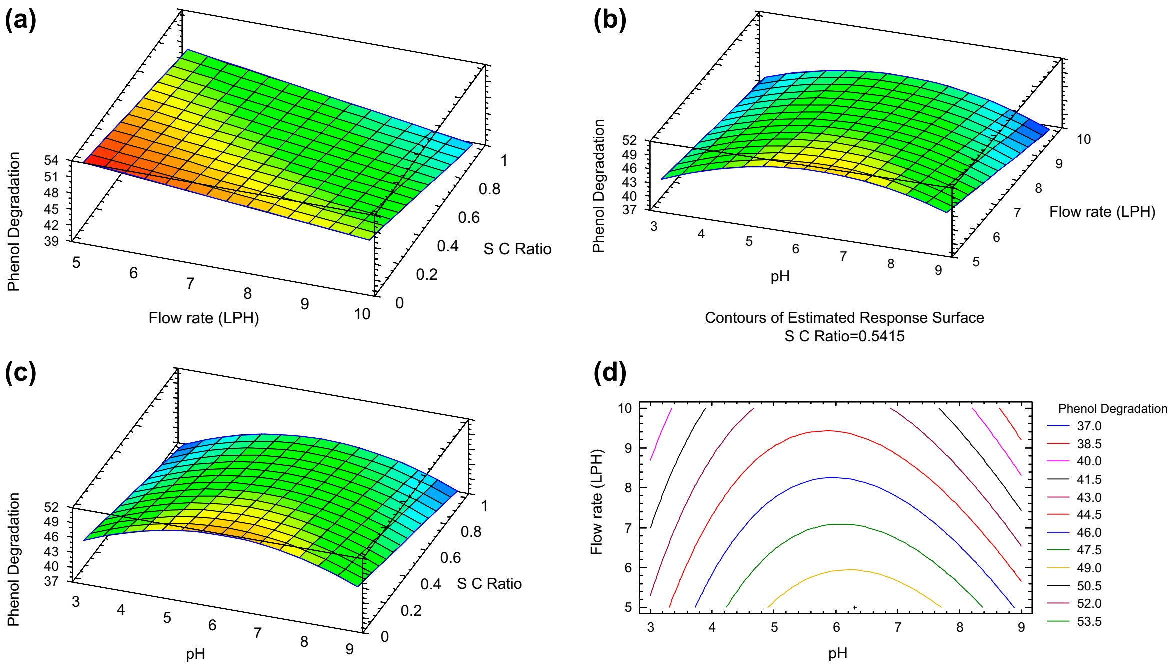

Fig. 4. (a) Interaction between flow rate and substrate-to-catalyst (S/C) ratio. (b) Interaction between pH and flow rate. (c) Interaction between pH and S/C ratio. (d) Contour plot of the interaction between flow rate and pH.

be attributed due to reduced relative availability of active sites on catalyst surface. Higher phenol degradation was achieved at higher catalyst loading, which corresponds to lower S/C ratio due to higher availability of the active sites. A similar observation was also manifested through different figures (Fig. 4(a) and (c)), which showed the response surface plot as a function of solution pH and S/S ratio. Photocatalytic processes involve formation, migration, and reaction of photogenerated radicals with organic compounds. At low substrate concentration, the active sites on TiO_2 surface were fully utilized. With increase in substrate concentration at constant catalyst loading, not all the molecules could get adsorbed on TiO_2 surface, and thus all the molecules could not get demineralized.

The effect of substrate concentration alone on degradation of phenol in solution has been given in Table 2. The runs were conducted at three initial phenol concentration (50, 125, and 200 ppm, respectively) keeping flow rate and catalyst loading fixed at 10 LPH and 400 ppm, respectively. The conversion was found to decrease with increase in phenol concentration. This could be due to the lesser availability of active sites for the photocatalysis reaction to take place.

4.3. Effect of pH

The effect of pH on the photocatalytic degradation efficiency of phenol by UV/TiO_2 process is one of the major factors affecting the rate of mineralization of various organic compounds [17]. The degradation of phenol was carried out under UV irradiation at different pH (3, 6, and 9). Effect of pH on phenol conversion is shown through the interaction plot between flow rate and pH, as depicted in Fig. 4(b). From the plot, it is evident there is an optimum pH that would result in maximum phenol conversion; which was obtained in mildly acidic to neutral region. The process of the photocatalytic degradation would involve radical oxidation, direct electron transfer, and surface sorption reaction [18]. At mildly acidic condition ($pH = 6$), the TiO_2 surface carries a net positive charge, while the phenols and the intermediates are basically negatively charged. This results in better adsorption and subsequent better degradation of phenol. However at stronger acidic condition ($pH = 3$), phenol degradation rate (i.e. conversion) got retarded, probably due to the presence of excess hydrogen ion in the system. At alkaline medium ($pH = 9$), formation

Table 2
Effect of substrate concentration on phenol conversion

Phenol concentration, ppm	Conversion (after 3h)
50	46.5 ± 1.8
125	40.3 ± 1.1
200	34.4 ± 0.8

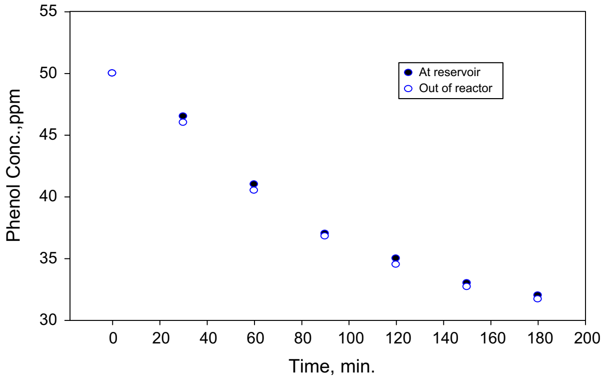

Fig. 5. Effect of sampling point on phenol degradation.

of OH radical, the main agent causing photocatalytic oxidation got retarded; Moreover in the vicinity of this pH, phenol became ionized (negatively charged) and repelled from the negatively charged surface of the adsorbent, TiO_2. Due to these causes, at higher pH, the adsorption of phenol on TiO_2 active sites decreased, thus lowering phenol degradation rate. Similar observation was also studied in Fig. 4(c) which is another response surface plot involving solution pH and S-C ratio. Whatever be the S-C ratio, the trend of phenol degradation percentage first increased up to a pH in the vicinity of 6–7 and then decreased.

4.4. Effect of sampling point

The influence of the sample point on phenol degradation was studied by collecting samples from two different sampling sources (Fig. 2), one at the outflow (2) of the reactor and the other from the reservoir (1). In Fig. 5, it was observed that the phenol concentration at these two points did not differ much though concentration at the outflow of reactor was slightly less compared to that from the reservoir. This could be due to the fact that the phenol solution coming out of the reactor, just after being exposed to UV radiation and subsequent degradation, contained lesser amount of phenol than that collected at reservoir at that instant. The solution coming out of UV reactor subsequently got mixed and homogenized with the entire volume of solution having slightly higher concentration of phenol. In this work, the conversion of phenol was calculated based on phenol concentration measured from the sampling port 2.

4.5. Kinetic study

The photocatalytic oxidation kinetics of many organic compounds has been modeled with the L–H equation, in which the adsorption properties of the substrate on the photocatalyst are also covered. This model was developed by Turchi and Ollis [19]. Phenol degradation rate at very dilute solution followed pseudo-first-order kinetics equation (11). The apparent rate constant was determined from the plot of ln (C_0/C) against time (Fig. 6). Linear least square technique was used to determine the slope of the straight line, and hence the apparent rate constant. From the linear regression analysis, the apparent rate constant is found to be 0.0028 min^{-1}, with a correlation coefficient of 0.98 indicating goodness of fit.

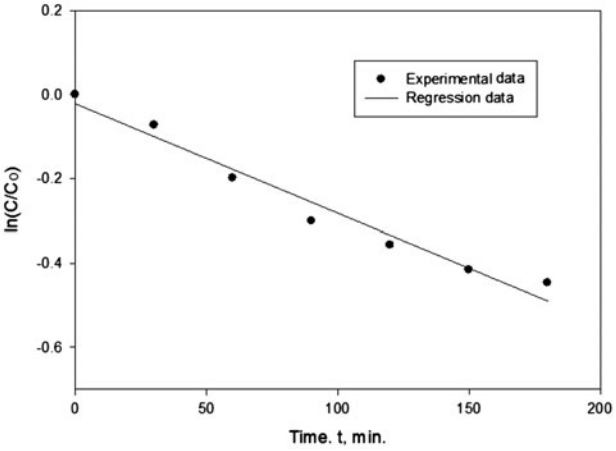

Fig. 6. Plot for determining kinetic constant for phenol degradation.

4.6. Improvement of water quality parameters

To study the improvement of water quality parameters, the COD and pH of phenol solution before and after photocalysis were measured and reported in Table 3. It has been found that a significant improvement of COD value has been achieved following photocatalysis.

In Fig. 7 the residual (errors) phenol conversion was plotted against the predicted phenol conversion. The random nature of the distribution of the residuals over and below the center line suggests that the model for phenol conversion is statistically significant.

5. Optimization of responses

The desirability function (DF) is widely used in RSM to determine a combination of variables to optimize multiple responses [20–22]. For each response *yk (xi)*, a DF *dk (yk)* assigns numbers between 0 and 1 to the possible values of *yk*, with *dk (yk)* = 0 representing

Table 3
pH and COD values before and after photocatalysis

Item		pH	COD (in ppm)
Phenol solution before photocatalysis	50 ppm	6.8	143 ± 5
	125 ppm	6.6	322 ± 12
	200 ppm	6.5	510 ± 15
Phenol solution after photocatalysis	50 ppm	7.0	30 ± 1
	125 ppm	6.9	93 ± 3
	200 ppm	6.9	142 ± 5

Table 4
Optimization results for the phenol conversion

	Variable factors	Optimum
Optimized coded level of variables	Flow rate	5.0
	S/C ratio	0.083
	pH	6.3
Predicted responses	Phenol conversion	52.81

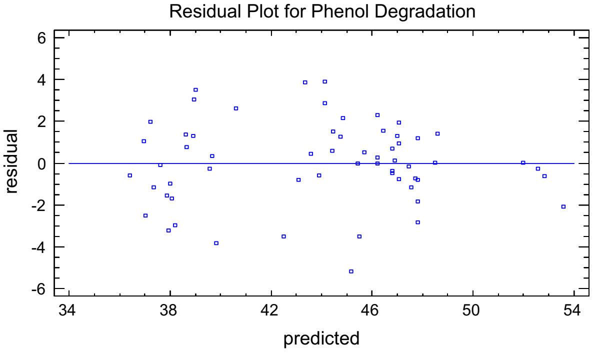

Fig. 7. Plot of residuals against predicted response of phenol conversion.

a completely undesirable value of *yk*, and *dk (yk)* = 1 representing a completely desirable or ideal response value. In addition a DF method finds operating conditions that provide the "most desirable" responses. It is based on the conduction of experiments and fitting of response models (*yk*) for all *k* responses, the definition of individual DFs for each response (*dk*), and the maximization of the overall desirability in comparison with controllable factors. For each response *yk (xi)*, a DF *dk (yk)* assigns numbers between 0 and 1. Depending on whether a particular response *yi* has to be maximized, minimized, or assigned to a target value, different DFs *dk (yk)* can be used [23]. The aim of this optimization was to find operating conditions corresponding to maximization of phenol conversion (degradation). Table 4 shows the optimal conditions corresponding to the maximum phenol conversion of 52.81%. It is very true that photocatalytic degradation is an energy-saving process and this was the perspective based on which this work was carried out to find an optimized and more efficient method for conversion of phenol into harmless products.

6. Conclusions

Present investigation revealed that heterogeneous photocatalysis using TiO_2 nanoparticles could be an effective method to degrade phenol, an organic pollutant in aqueous solution. The performance of the indigenous UV annular reactor was found to be satisfactory in mineralization of phenol in aqueous solution. This photocatalytic process proved to be an efficient and low-energy-intensive method. Influences of several parameters like flow rate, pH, substrate-to-catalyst ratio, and sampling point on degradation of phenol were studied and the optimum parameters were determined based on RSM. It was observed that for phenol in aqueous solution, the maximum conversion of 52.81% could be achieved under the following conditions: flow rate: 5.01LPH, S/C ratio: 0.083 with pH 6.3. The kinetics of photocatalytic removal of phenol followed the L–H model, with apparent first-order kinetic. Higher conversion could possibly be achieved with greater light intensity, and using sonolysis along with UV/TiO_2 AOP process.

Acknowledgments

The work reported in this article is part of an Indo-Korean project (vide sanction letter No. INT/Korea/P-11 dated 23 August, 2011), funded in India by the Department of Science & Technology (Government of India). The project involves collaboration between Gwangju Institute of Science & Technology (GIST), Gwangju, Korea, and Jadavpur University, Kolkata, India. Accordingly, the contributions of DST (India) are gratefully acknowledged.

Nomenclature

h_v — energy
$e^-_{cb}\,h^+_{vb}$ — electron-hole pair
X — conversion
C_0 — initial concentration
C — final concentration
θ — fractional coverage
K — equilibrium constant
k_r — true rate constant
k_{app} — apparent rate constant
t — time
CCD — central composite designs
SCD — small composite designs
RSM — response surface methodology

References

[1] N.A. Laoufi, D. Tassalit, F. Bentahar, The degradation of phenol in water solution by TiO_2 photocatalysis in a helical reactor, Global Nest J. 10 (2008) 404–418.

[2] R.W. Matthews, Purification of water with near UV illuminated suspensions of titanium dioxide, Wat. Res. 24 (1990) 653–660.

[3] O.K. Mahadwad, P.A. Parikh, R.V. Jasra, C. Patil, Photocatalytic degradation of reactive black-5 dye using TiO_2 impregnated ZSM-5, Bull. Mater. Sci. 34(3) (2011) 551–556.

[4] A. Hosseinnia, M. Keyanpour-Rad, M. Pazouki, Photocatalytic degradation of organic dyes with different chromophores by synthesized nanosize TiO_2 particles, World Appl. Sci. J. 8 (2010) 1327–1332.

[5] S.P. Devipriya, S. Yasadharan, Photocatalytic degradation of phenol in water using TiO_2 and ZnO, J. Environ. Biol. 31 (2010) 247–249.

[6] M.E. Kurtoglu, T. Longenbach, Y. Gogotsi, Preventing sodium poisoning of photocatalytic TiO_2 films on glass by metal doping, Int. J. Appl. Glass Sci. 2 (2011) 108–116.

[7] S.A. Jame, A.K.M. Rashidul Alam, A.N.M. Fakhruddin, M.K. Alam, Degradation of phenol by mixed culture of locally isolated pseudomonas species, J. Biorem. Biodegrad. 1 (2010) 1–4.

[8] J. Guélou, J. Barrault, J. Fournier, J.M. Tatibouët, Active iron species in the catalytic wet peroxide oxidation of phenol over pillared clays containing iron, Appl. Catal., B: Environ. 44 (2003) 1–8.

[9] D.H. Bremner, A.E. Burgess, D. Houllemare, K.C. Namkung, Phenol degradation using hydroxyl radicals generated from zero-valence iron and hydrogen peroxide, Appl. Catal., B: Environ. 63 (2006) 15–19.

[10] G.E.P. Box, K.B. Wilson, On the experimental attainment of optimum conditions, J. Royal Stat. Soc. Series B 13 (1951) 1–45.

[11] N.R. Draper, D.K.J. Lin, Small responce surface designs, Technometrics 32 (1990) 195–202.

[12] S.D. Ba, I.H. Boyacı, Modeling and optimization I: Usability of response surface methodology, J. Food Eng. 78 (2007) 836–845.

[13] C.F. Mandenius, A. Brundin, Bioprocess optimization using design-of-experiments methodology, Biotechnol. Progr. 24 (2008) 1191–1203.

[14] D.C. Montgomery, Design and Analysis of Experiments, Wiley, New York, NY, 2001.

[15] J.M. Herrmann, Heterogeneous photocatalysis: fundamentals and applications to the removal of various types of aqueous pollutants, Catal. Today 53 (1999) 115–129.

[16] L. Gámiz-Gracia, L. Cuadros-Rodríguez, E.J. Almansa-López, J.M. Soto-Chinchilla, A. García-Campaña, Use of highly efficient Draper–Lin small composite designs in the formal optimisation of both operational and chemical crucial variables affecting a FIA-chemiluminescence detection system, Talanta 60 (2003) 523–534.

[17] K.H. Wang, H.Y.H. Isieh, C.H. Wu, C.H. Chang, The pH and anion effects on the heterogeneous photocatalytic degradation of o-methylbenzoic acid in TiO_2 aqueous suspension, Chemosphere 40 (2000) 389–394

[18] M.A. Fox, M.T. Dulay, Heterogeneous photocatalysis, Chem. Rev. 93 (1993) 341–357.

[19] C.S. Turchi, D.F. Ollis, Photocatalytic degradation of organic water contaminants: Mechanisms involving hydroxyl radical attack, J. Catal. 122 (1990) 178–192.

[20] M. Cheryan (Ed.), Ultrafiltration and Microfiltration Handbook, Technomic Publishing, Pennsylvania, USA, 1998.

[21] W.M. Lu, C.C. Lai, K.J. Hwang, Constant pressure filtration of submicron particles, Sep. Technol. 5 (1995) 45–53.

[22] S. Chakraborty, E. Drioli, L. Giorno, Development of a two separate phase submerged biocatalytic membrane reactor for the production of fatty acids and glycerol from residual vegetable oil streams, Biomass Bioenergy 46 (2012) 574–583.

[23] C. Tien, B.V. Ramarao, On analysis of cake formation and growth in cake filtration, J. Chin. Inst. Chem. Eng. 37(1) (2006) 81–94.